

Supplementary Information:

Single-cell RNA sequencing identifies distinct mouse medial ganglionic eminence cell types

Ying-Jiun Jasmine Chen^{1,4}, Brad Friedman^{2,4}, Connie Ha¹, Steffen Durinck^{1,2}, Jinfeng Liu², John Rubenstein³, Somasekar Seshagiri¹ and Zora Modrusan^{1*}

¹Department of Molecular Biology and ²Department of Bioinformatics and Computational Biology, Genentech, 1 DNA Way, South San Francisco, CA 94080; ³Department of Psychiatry, University of California San Francisco, CA 94158.

⁴Co-first author

*Correspondence: modrusan.zora@gene.com

Supplemental Figure Legends

Figure S1. Validation of E11.5 MGE gene expression and the two major cell populations, proliferating neural progenitors (n=22), and immature neurons (n=31), by single-cell quantitative PCR. Two proliferating neural progenitor cells also express markers from immature neurons (marked with *).

Figure S2. Correlation of gene expression differences between the quiescent vs. replicating cells in the human fetal cortex and between immature neurons vs. proliferating neural progenitors in the mouse E11.5 MGE. Each dot represents a gene. Only genes with more than 4 times of fold changes, and with adjusted p value no more than 0.05 for both comparisons (on X and Y axis) are shown.

Figure S3. (A) MGE cells from different ages (E11.5 to E17.5, n=225) were classified either as immature neurons (n=133) or proliferating progenitors (n=74) based on the expression level of top 100 differentially expressed genes between the two identified E11.5 MGE cell types. A few cells did not express either of the gene sets were marked as “others” (n=18). (B) Number of cells for three different cell phenotypes including proliferating (E11.5 n=37, E13.5 n=24, E15.5 n=12, E17.5 n=1), immature (E11.5 n=58, E13.5 n=20, E15.5 n=39, E17.5 n=16) and others (E11.5 n=1, E13.5 n=4, E15.5 n=12, E17.5 n=1). at each MGE age determined from differential gene expression analysis shown in A. (C) Percentage of immature neurons across different embryonic ages. Error bars represent 95% confidence intervals for binomial probabilities. P values were calculated by Fisher’s exact test.

Figure S4. (A) Unsupervised gene-sample heatmap for proliferating neural progenitors (n=70). Each row represents one gene and each column represents one cell. The top part of the heatmap came from the PCA analysis and genes were ordered by unsupervised clustering. VZ (n=34) and SVZ (n=35) cells are defined based on the differential expression of Hes1, Gad2

and *Dlx2*. One E13.5 cell (to the right of SVZ cells) has low numbers of detected genes and was not defined as either a VZ or SVZ cell. Five distinct gene blocks based on gene expression patterns were marked as i, ii, iii, iv, v on the right. The cell on the farthest right was excluded for further characterization as it did not resemble either cell type. (B) Unsupervised gene-sample heatmap for immature neurons (n=133). Four sub-populations were indicated on the top: MGE-derived neurons (MGE, n=60), cells with low numbers of genes detected (L#G, n=8), mix of MGE and LGE-derived neurons (MGE and LGE, n=49), LGE-derived neurons (LGE, n=16). Blocks of genes with expression correlated with LGE neurons, mitochondria and ribosomal genes, genes with neuronal functions or neuronal markers, genes whose functions are transcriptional regulators, nuclear RNA regulators and chromatin modifier and/or are basal ganglion patterning genes and genes associated with MGE-derived neurons are indicated on the right as vi, vii, viii, ix, x. The L#G group was omitted from Fig 4B for visualization purposes.

Figure S5. (A) Single-cell RNA-seq from juvenile mouse cortex and hippocampus (GSE60361) were used to generate cell type-specific markers. (B) Marker gene expression analyses identified putative non-neuronal cell types (marked by boxes) including 4 astrocytes, 5 ependymal cells, 4 microglia, 1 endothelial, 3 vascular smooth muscle cells (Vsmc), 1 pyramidal neurons and 7 oligodendrocytes.

Figure S6. (A) Gene-sample heatmap showing genes that were enriched in three astrocyte/ependymal, four microglia, and four endothelial/vascular smooth muscle cells identified in the mouse MGE and their level of expression in each cell type (cell types indicated on the top). One hundred and thirty-three immature neurons and sixty-six proliferating neural progenitors of the MGE were also shown in each column but with narrower width relative to the 11 non-neuronal cells. (B and C) Gene expression analysis using the same genes from A and comparing with other public datasets from sorted mouse cortical cells (GSE52564) and from

juvenile hippocampal and cortical single cells (GSE60361). Some of the genes that were specific for each cell type were indicated on the left in (A) and on the right in (C).

Figure S7. Quality control metrics used to process sequencing reads from (A) *in vivo* MGE cells at E11.5 (blue, n=96), E13.5 (red, n=48), E15.5 (orange, n=63) and E17.5 (purple, n=18) (B) *in vitro* undifferentiated ES cells (dark blue, n=21), unsorted (grey, n=39) and GFP sorted (green, n=53) differentiated ES cells. Bar graphs from top to bottom illustrate numbers of total reads, percent of uniquely mapped reads, percent reads mapped to ribosomal RNA and mitochondrial RNA and the percentage and total number of genes detected (bottom right).

Figure S8. Distribution of single cells (represented by individual circles, n=403) from *in vitro* system based on the percentage of genes with at least one read (X axis) and the percentage of reads aligning to a single gene (Y axis). Single cells used for current study (n=113 for *in vitro* system) were selected based on >10% of genes detected and more than 2M reads.

Figure S1

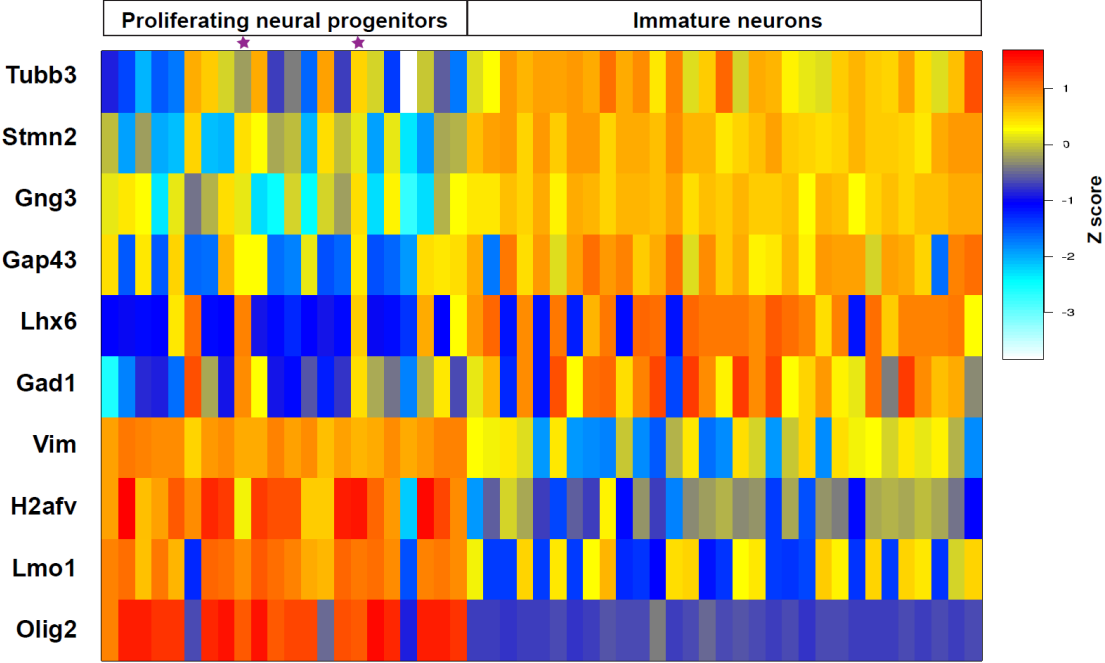


Figure S2

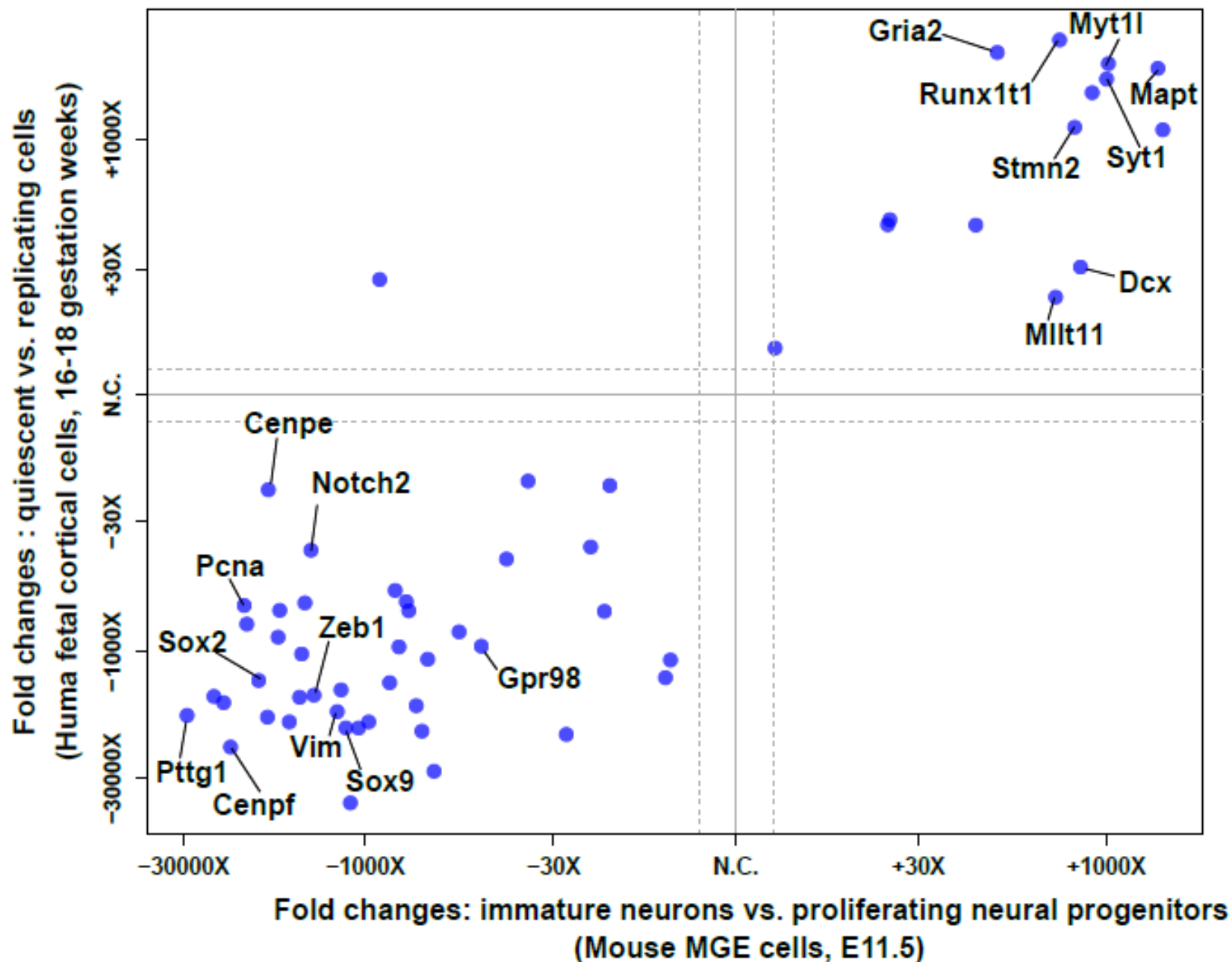
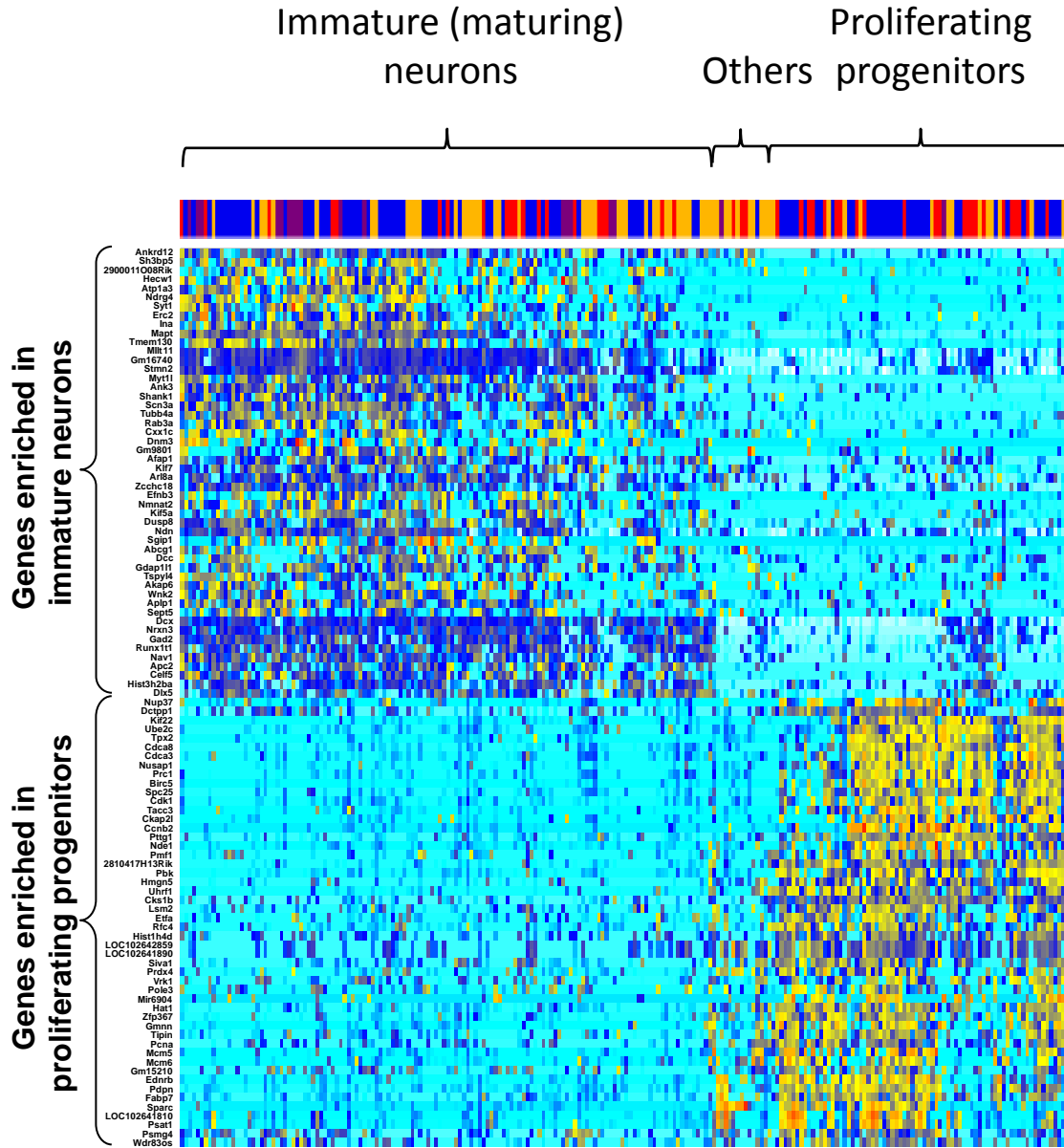
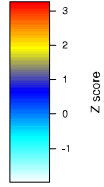
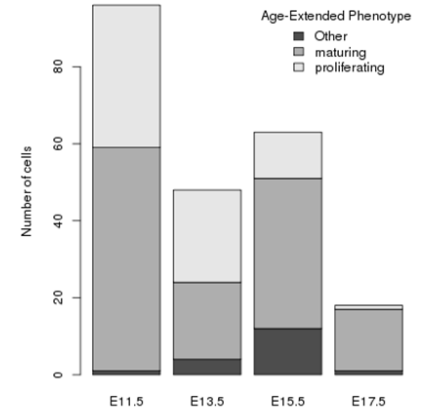


Figure S3

A



B



C

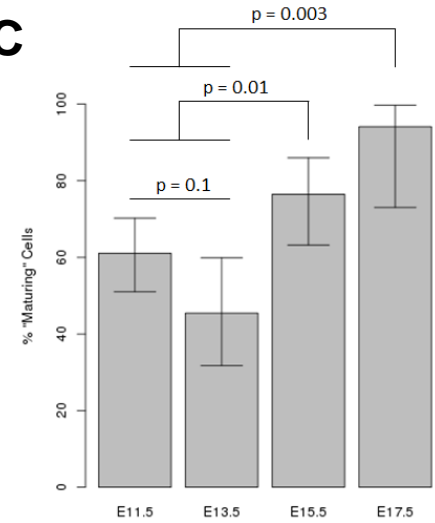


Figure S6

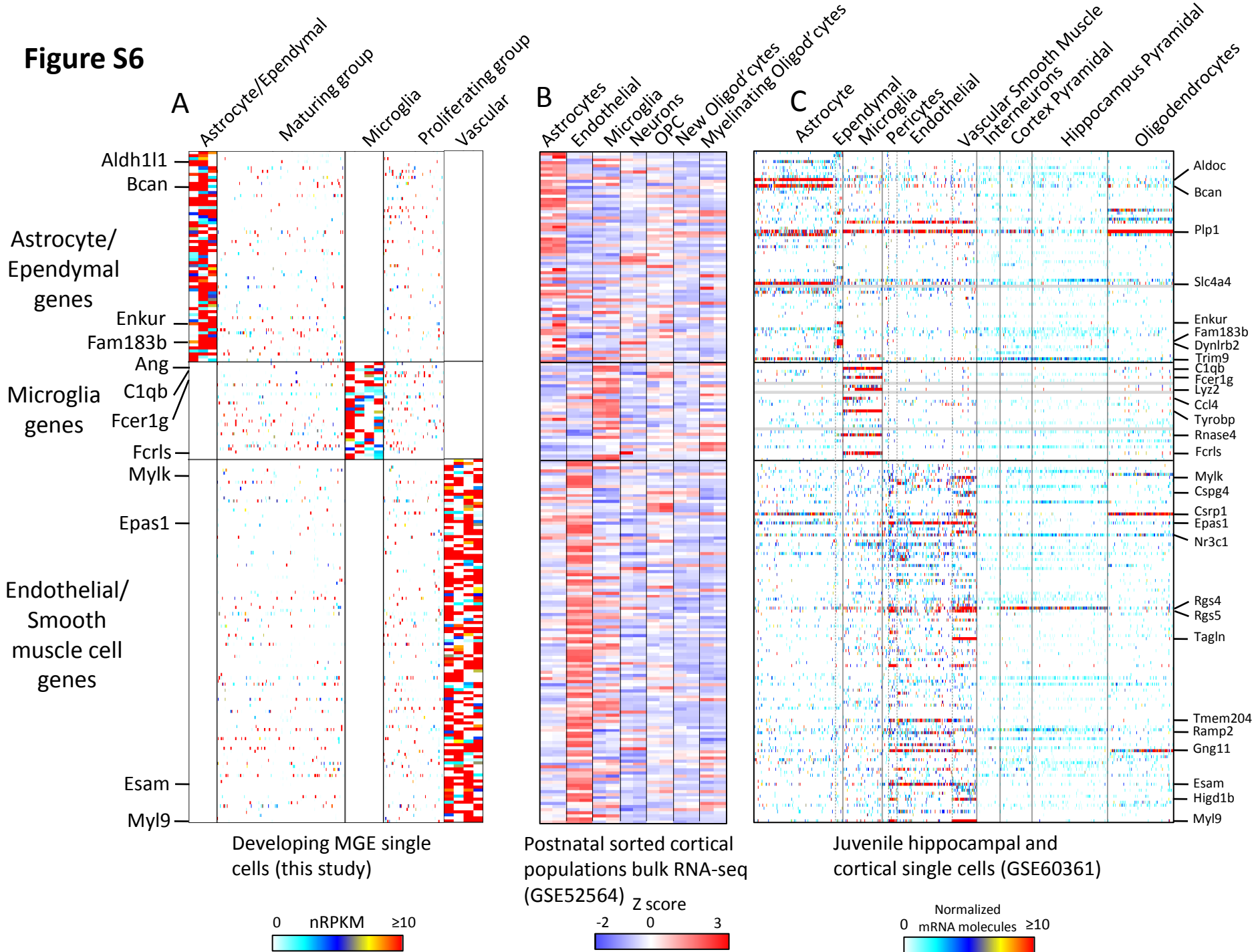
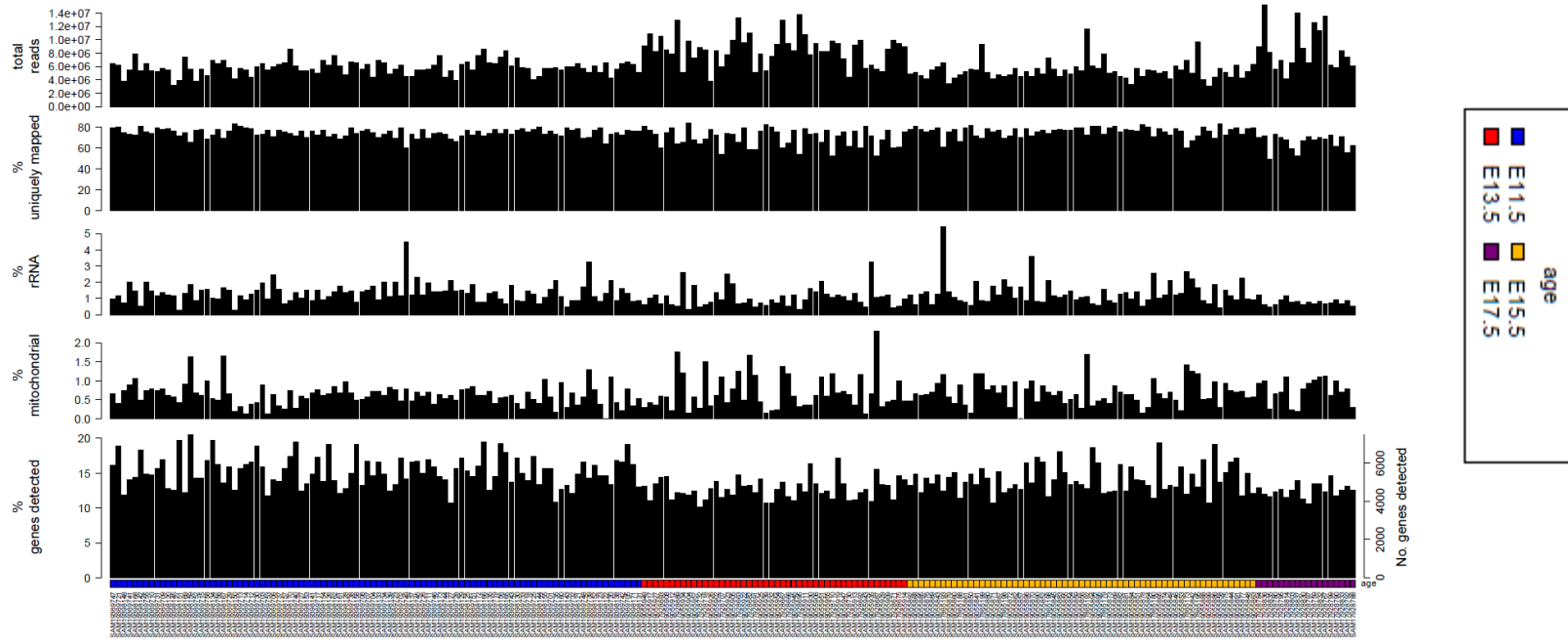


Figure S7

A



B

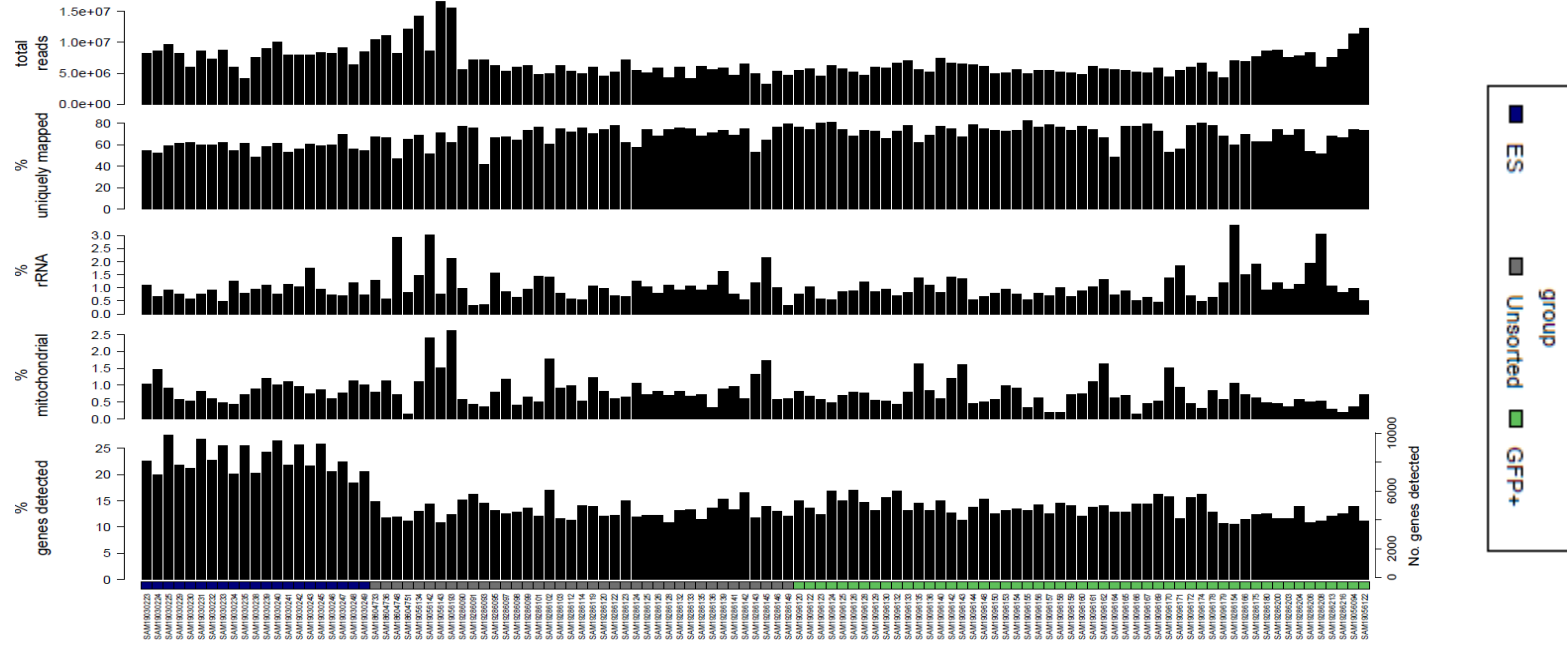


Figure S8

